HHS Public Access

Author manuscript

Thromb Haemost. Author manuscript; available in PMC 2020 August 01.

Published in final edited form as:

Thromb Haemost. 2020 February ; 120(2): 289–299. doi:10.1055/s-0039-3400959.

Ly6C^{Lo} Monocyte/Macrophages are Essential for Thrombus Resolution in a Murine Model of Venous Thrombosis

Andrew Scott Kimball[1,*], **Andrea Tara Obi**[1,*], **Catherine E. Luke**[1], **Abigail R. Dowling**[1], **Qing Cai**[1], **Reheman Adili**[2], **Hannah Jankowski**[1], **Matthew Schaller**[3], **Michael Holinstadt**[2], **Farouc A. Jaffer**[4], **Steven L. Kunkel**[5], **Katherine A. Gallagher**[1], **Peter K. Henke**[1]

[1]Department of Surgery, Conrad Jobst Vascular Research Laboratories, University of Michigan, Ann Arbor, Michigan, United States

[2]Department of Pharmacology, University of Michigan, Ann Arbor, Michigan, United States

[3]Division of Pulmonary Critical Care Medicine, University of Florida, Gainesville, Florida, United States

[4]Department of Cardiology, Massachusetts General Hospital, Boston, Massachusetts, United States

[5]Department of Pathology, University of Michigan, Ann Arbor, Michigan, United States

Abstract

Venous thrombosis (VT) resolution is a complex process, resembling sterile wound healing. Infiltrating blood-derived monocyte/macrophages (Mo/MΦs) are essential for the regulation of inflammation in tissue repair. These cells differentiate into inflammatory (CD11b^{+}Ly6C^{Hi}) or proreparative (CD11b^{+}Ly6C^{Lo}) subtypes. Previous studies have shown that infiltrating Mo/MΦs are important for VT resolution, but the precise roles of different Mo/MΦs subsets are not well understood. Utilizing murine models of stasis and stenosis inferior vena cava thrombosis in concert with a Mo/MΦ depletion model (CD11b-diphtheria toxin receptor [DTR]-expressing mice), we examined the effect of Mo/MΦ depletion on thrombogenesis and VT resolution. In the setting of an 80 to 90% reduction in circulating CD11b^{+}Mo/MΦs, we demonstrated that Mo/MΦs are not essential for thrombogenesis, with no difference in thrombus size, neutrophil recruitment, or neutrophil extracellular traps found. Conversely, CD11b^{+}Mo/MΦ are essential for VT resolution. Diphtheria toxoid (DTx)-mediated depletion after thrombus creation depleted primarily CD11b^{+}Ly6C^{Lo} Mo/MΦs and resulted in larger thrombi. DTx-mediated depletion did not alter CD11b^{+}Ly6C^{Hi} Mo/MΦ recruitment, suggesting a protective effect of CD11b^{+}Ly6C^{Lo} Mo/MΦs in VT resolution. Confirmatory Mo/MΦ depletion with clodronate lysosomes showed a similar phenotype, with failure to resolve VT. Adoptive transfer of CD11b^{+}Ly6C^{Lo} Mo/MΦs into Mo/MΦ-depleted mice reversed the phenotype, restoring normal thrombus resolution. These findings suggest that CD11b^{+}Ly6C^{Lo} Mo/MΦs are essential for normal VT resolution, consistent with the known proreparative function of this subset, and that further study of Mo/MΦ subsets may identify targets for immunomodulation to accelerate and improve thrombosis resolution.

Address for correspondence Peter K. Henke, MD, 1500 East Medical Center Drive, 5463 Cardiovascular Center, Ann Arbor, Michigan 48109, United States (henke@med.umich.edu).

*Shared authorship.

Keywords

venous thromboembolism; thrombosis; macrophages; monocytes; inflammation

Introduction

Deep venous thrombosis (DVT) is a significant health care problem in the United States, with over 250,000 patients affected yearly, and at least 200,000 diagnosed with pulmonary embolism (PE).[1] The cornerstone of DVT therapy is anticoagulation.[2] While effective, the bleeding risks of all Food and Drug Administration-approved anticoagulants, including direct oral anticoagulants, are significant and many patients have contraindications to anticoagulation.[3,4] Nonanticoagulant therapies represent a potential ideal strategy to improve DVT outcomes.

Venous thrombosis (VT) is an inflammatory process.[5-8] Leukocytes, chemokines, plasminogen activators, matrix metalloproteinases (MMPs), and proinflammatory cytokines are all involved in the process of VT resolution and vein wall injury.[5,7,9-13] This process resembles sterile wound healing,[14] with phases of neutrophil (polymorphonuclear [PMN]) and monocyte/macrophage (Mo/MΦ) influx, followed by fibrosis.

Mo/MΦs are the primary leukocyte involved in VT resolution,[5,7,15,16] by clearance of apoptotic and necrotic cells and matrix debris,[14,17-19] profibrinolytic activity, and promotion of thrombus neovascularization.[11,20,21] Mo/MΦ are classified by their inflammatory or anti-inflammatory functions.[22] For example, cell surface $CD11b^{+}Ly6C^{Hi}$,$CCR2^{2+}$,$CX3CR1^{+}$ antigen expression characterize classically activated, or proinflammatory Mo/MΦs. Conversely, cell surface $CD11b^{+}Ly6C^{Lo}$, $CCR2^{-}$, CX_3CR1^{2+} antigen expression, characterize alternatively activated Mo/MΦs, with prohealing and inflammation-resolving activities.

Studying in vitro skewing of Mo/MΦs into pure M_1 (proinflammatory) or M_2 (anti-inflammatory) phenotypes is not translatable to in vivo leukocytes.[23-25]

Herein, we show that depletion of circulating $CD11b^{+}Ly6C^{+}$ Mo/MΦs impairs VT resolution, is associated with significantly reduced $CD11b^{+}Ly6C^{Lo}$ but not CD11b + $Ly6C^{Hi}$ subtypes within the venous thrombus and adjacent vein wall, and resolution can be rescued with adoptive transfer of $CD11b^{+}Ly6C^{Lo}$ Mo/MΦs.

Materials and Methods

Mice

Wild-type (WT) C57BL/6J, CD11b-DTR (C57BL/6 background), and mTmG mice (*Gt(ROSA)26Sor*$^{tm4(ACTB-tdTomato,-EGFP)Luo/J}$) were obtained from the Jackson Laboratory (Bar Harbor, Maine, United States). Tail clipping and standard polymerase chain reaction genotyping verified fidelity. All animals underwent procedures between 8 and 10 weeks of age with institutional animal care and use committee approval.

Venous Thrombosis Mouse Models

VT was formed via (1) generation of stasis by inferior vena cava (IVC) ligation or (2) generation of stenosis via partial ligation of the IVC.[26] Following laparotomy, VT was induced by infrarenal IVC ligation with a single 7–0 prolene suture with concurrent cauterization of lumbar and side branches; or in the case of the stenosis model, a prolene was tied around a 30-gauge needle adjacent to the IVC to produce turbulent flow and stenosis with side branch ligation, but without lumbar branch cauterization.[26]

NaCl and Diphtheria Toxin Injections

Diphtheria toxin (*Corynebacterium diphtheria*, DTx) was obtained from Enzo Life Sciences, Inc. (Farmingdale, New York, United States), and 10 ng/g doses were injected intraperitoneal into CD11b-diphtheria toxin receptor (DTR) mice or WT mice.[27] CD11b-DTR mice were either injected 24 hours prior to IVC ligation (in experiments evaluating thrombogenesis) or were injected approximately 48 hours after IVC ligation and every 48 hours thereafter in experiments evaluating thrombosis resolution. Control CD11b-DTR mice were injected with equal volumes of 0.9% normal saline (NaCl) based on weight (10 μL/g).

IVC Harvest and Weight to Length Analysis

Mice were euthanized on postoperative days 1, 2, and 8. Following euthanasia, the IVC/thrombus was harvested from the abdominal cavity en bloc with bilateral iliac veins. The thrombus was then measured (cm) and weighed (g) for weight to length analysis.[9-11] For flow cytometry and histology, the IVC/thrombus was kept intact and either fixed in formalin for histology, or placed in Roswell Park Memorial Institute (RPMI) medium for cell extraction for flow cytometry.

Cell Extraction for Flow Cytometry

IVC/thrombus samples placed in RPMI were minced with sharp Iris scissors and then enzymatically digested with Liberase (Sigma-Aldrich) and DNase I (Sigma-Aldrich) at 30° C for 30 minutes. After enzymatic digestion, the reaction was stopped with RPMI + fetal bovine serum (FBS) and samples were plunged with a 3 mL syringe ×20 and filtered through a 100-μm filter. The resultant single cell suspensions were then washed in phosphate-buffered saline (PBS) and resuspended for surface staining. Peripheral blood was drawn via submandibular vein puncture or cardiac puncture and collected in ethylenediaminetetraacetic acid (EDTA)-coated tubes, red blood cells (RBCs) were lysed with RBC lysis buffer for 5 to 10 minutes at room temperature, remaining cells were washed with PBS, and resuspended for surface staining.

Flow Cytometry/Fluorescent-Activated Cell Sorting

Single cell suspensions were plated in 96-well plates for flow staining. Cells were first stained with a Fixable LIVE/DEAD viability dye (Molecular Probes by Life Technologies; Ref. L34959; 1:1,000 dilution). Following viability staining, cells were washed in PBS and resuspended in flow buffer (PBS, FBS, NaN3, HEPES). Fc receptors were then blocked with anti-CD16/32 (BioXCell, Cat. CUS-HB-197, 1:200 dilution) for 10 minutes. Monoclonal antibodies for surface staining included: anti-CD3 (Biolegend, Cat. 100304, 1:400 dilution),

anti-CD19 (Biolegend, Cat. 115504,1:400 dilution), anti-Ter-119 (Biolegend, Cat. 116204, 1:400 dilution), anti-NK1.1 (Cat. 108704, 1:400 dilution), anti-Ly6G (Biolegend, Cat. 127604, 1:400 dilution), anti-CD11b (Biolegend, Cat. 101230, 1:400 dilution), anti-Ly6C (Biolegend, Cat. 128035, 1:400 dilution), and anti-F4/80 (Biolegend, Cat. 123121, 1:400 dilution) as previously described.[25] Following surface staining, cells were washed, and biotinylated antibodies were labeled with streptavidin–fluorophore (Biolegend, Cat. 405208, 1:1,000 dilution). Stained samples were then washed twice in flow buffer and acquired on a 3-Laser Novocyte Flow Cytometer (Acea Biosciences) or fluorescent-activated cell sorting (FACS) on a FACS Aria III Flow Sorter. FACsDiva Software (BD Biosciences) was used for flow sorting, and FlowJo version 10.0 (Tree Star) was used for flow cytometric analysis. Back gating of cell populations was performed to verify gating and purity.

Hematology

Evaluation of complete blood cell count was performed as previously described.[28,29] A total of 100 uL of blood via submandibular was drawn into an EDTA Microvette tube (Sarstedt) or 500 μL of blood was drawn via cardiocentesis (if terminal procedure). An aliquot of 10 μL was used for analysis on an Element HT5 hematology analyzer (Heska), including white blood cell count, differential count (neutrophils, monocytes, and lymphocytes), RBC count, platelet count, and hematocrit.

Histochemistry

Fresh tissue (IVC with thrombus intact) was fixed in 10% buffered formaldehyde for approximately 2 hours, transferred to 70% ethanol, and embedded in paraffin and mounted to slides in 5 μm tissue sections. Slides were deparaffinized and rehydrated in xylene and graded ethanol. For immunohistochemistry, heat-mediated sodium citrate method was used for antigen retrieval. Nonspecific binding sites were blocked with species-specific serum and antibody was applied for activated neutrophils using Ly6G (1:3000, BD Pharmingen, San Diego, California, United States), for proreparative Mo/MΦs using Arg1 (NBP1–54621, 1:1,000, Novus Biologicals, Centennial, Colorado, United States), and for recanalization channels using von Willebrand factor (vWF) (ab6994, 1:500, Abcam, Cambridge, Massachusetts, United States) staining. A peroxidase species-specific kit was used for secondary antibody. ImmPACT diaminobenzidine peroxidase substrate was applied, tissues were counterstained with hematoxylin, and cover slipped (Vector Laboratories, Inc., Burlingame, California, United States). Cells were quantified in a blinded fashion, with positive cells in five to eight high-power fields (magnification, 1,000×) radially around the IVC wall were counted and totaled.

Picro-Mallory stain from StainsFile (http://stainsfile.info/StainsFile/stain/fibrin/picro-mallory-2.htm) was performed on deparaffinized and rehydrated tissue slides. Fibrin, connective tissue (collagen), and erythrocytes were quantitatively analyzed using ImageJ (National Institutes of Health [NIH]).

Terminal deoxynucleotidyl transferase dUTP nick end labeling (TUNEL) staining was performed to formaldehyde fixed, deparaffinized tissue slides with Promega DeadEnd Fluorometric TUNEL system kit according to manufacturer’s instructions. This was

followed with the addition of a 500-nM propidium iodide for 1 to 5 minutes as previously described.[30] Images were taken on Nikon E400 and analyzed with ImageJ software for percent area of each color at 100×. Ten pictures were taken per animal and analyzed of each vein wall with clot, and averaged for each mouse.

Western Immunoblotting

Protein levels of fibrin, citrullinated histone-3 (cit-H_3), plasminogen, and β-actin were measured by Western blot from thrombus tissue. Protein was isolated using RIPA buffer (ThermoScientific) with dissolved complete ULTRA mini proteinase tablets (Roche). Proteins were electrophoretically separated on NuPAGE 4–12% Bis-Tris gels (Invitrogen) and transferred onto polyvinylidene difluoride membranes (Millipore). Nonspecific binding was blocked with starting block (TBS) blocking buffer (ThermoScientific). Antibodies included: anti-H_3 (1/500 dil., Abcam), anti-fibrin (clone 59d8, 1/1,000 dil., gift of Dr. Charles Esmon), anti-β-actin (Santa Cruz, 1:20,000), anti-α5-integrin (Abcam, 1:500), anti-fibronectin (Abcam, 1:500), anti-laminin (Abcam 1:500), anti-uPAR (R&D Systems, 1:500), anti-interferon (IFN)-γ (Abcam 1:500), and anti-plasminogen (Gene Tex, 1:1,000). Immunoreactive bands were visualized with SuperSignal West Pico Chemiluminescent Substrate (ThermoScientific), and densitometry was performed using ImageJ software. Optical densities were summed and normalized to β-actin.

Enzyme-Linked Immunosorbent Assays

Thrombi were homogenized and sonicated and then centrifuged at 13,200 g for 30 minute. The supernatant was collected for enzyme-linked immunosorbent assay analysis. Thrombin–antithrombin (TAT) complex, plasminogen (My BioSource, San Diego, California, United States), was determined by commercially available kits according to the manufacturer's instructions. Plates were read on a Synergy 2 Plate Reader (Biotek, Winooski, Vermont, United States) at 450 nm.

Magnetic-Activated Cell Sorting for Adoptive Transfer

For adoptive transfer experiments, magnetic-activated cell sorting (MACS) was used to further isolate $CD11b^+$ cells from donor animals to assure purity and simplify FACS. C57BL/6J and mTmG spleens were isolated from donor animals, immersed in RPMI, crushed and filtered through a 100-μm filter, passed through a Ficoll gradient, washed, and resuspended in MACS buffer. Single cell suspensions were then incubated with fluorescein isothiocyanate-labeled anti-CD3, anti-CD19, and anti-Ly6G (Biolegend) followed by antifluorescein isothiocyanate microbeads (Miltenyi Biotec; Cat. 130–042–401, 130–049–601). The suspension was then passed through a MACS column and flow-through was incubated with anti-CD11b microbeads (Miltenyi Biotec; Cat. 130–049–601). The flow-through was then passed through a separate column, flow-through eliminated, and then the column was purged to isolate non-neutrophil, non-T cell, non-B cell, and $CD11b^+$ cells for expedited FACS.

Adoptive Transfer

Blood and splenic leukocytes from C57BL/6J and mTmG mice were passed through a Ficoll gradient, MACS sorted, and FACS sorted as described above. Isolated $CD11b^{+}Ly6C^{Lo}$ Mo/MΦs were then diluted in RPMI and approximately 100,000 cells/mouse were adoptively transferred via tail vein injection into CD11b-DTR mice treated with either DTx or NaCl 72 hours post-IVC ligation and 24 hours postinjection. For controls, an equal volume of RPMI was injected via tail vein. Confirmation of adoptive transfer was performed with flow cytometry as described above.

Statistical Analysis

GraphPad Prism software version 6.0 was used to analyze the data. Data are presented as the mean ± the standard deviation. Data was first analyzed for normal distribution and then statistical significance between multiple groups was determined using one-way analysis of variance followed by Newman–Keuls post hoc test. For all other single group comparisons if data passed normality test, we used two-tailed Student's *t*-test. Otherwise data were analyzed using Mann–Whitney *U*-test. All data are representative of at least two independent experiments. A *p*-value of less than or equal to 0.05 was considered significant.

Results

$CD11b^{+}Ly6C^{Hi}$ Mo/MΦs Rapidly Accumulate following VT and Transition to $CD11b^{+}Ly6C^{Lo}$ Macrophages

The process of VT resolution resembles sterile wound healing in which Mo/MΦ influx plays a dichotomous role by both providing aid in thrombus resolution and by causing tissue destruction after VT. Thrombus resolution commences after day 4 involving multiple processes including fibrinolysis, neovascularization, and matrix changes.[5,7] Mo/MΦs are highly plastic in acute inflammation; a growing body of literature supports that an imbalance of pro- and anti-inflammatory Mo/MΦs may contribute significantly to several sterile inflammatory conditions.[31-34] To identify the kinetics of Mo/MΦ subsets after VT in our model, mice underwent induction of VT via IVC ligation and thrombosed vena cavas were processed for flow cytometry at days 1, 3, and 8 postoperatively. The gating strategy removed nonviable cells, doublets, and neutrophils ($Ly6G^{-}$) and selected $CD11b^{+}$ cells (►Fig. 1A). Proportions of identifiable $CD11b^{+}Ly6C^{Hi}$ and $CD11b^{+}Ly6C^{Lo}$ cells were determined as shown in the density plot (►Fig. 1B). Consistent with data from other organ systems,[25,33] and more recent data in VT from Schönfelder et al,[35] we found two distinct populations of $CD11b^{+}Ly6C^{Hi}$ and $CD11b^{+}Ly6C^{Lo}$ cells at each time point post-VT. The relative proportions of these myeloid subsets changed over time: within the first 72 hours $CD11b^{+}Ly6C^{Hi}$ cells predominated; however, by day 8 $CD11b^{+}Ly6C^{Lo}$ cells dominated. In addition to confirming the natural history of Mo/MΦ influx to the thrombosed vein, these data demonstrate the ability to track and compare these two cellular populations over time (►Fig. 1C).

CD11b-DTR Mice Injected with DTx have Selective Depletion of Peripheral Blood Monocyte/Macrophages without Significant Effects on Circulating Neutrophils

To determine the role that Mo/MΦs have during the pathophysiology of VT, we used a transgenic mouse with DTR expression restricted to CD11b+ cells (CD11b-DTR). CD11b-DTR mice were injected with either NaCl or DTx (10 ng/g) one time. Previous reports have shown that similar doses of DTx selectively deplete macrophages and circulating monocytes without altering neutrophils or lymphocytes.[36] To verify that macrophages were depleted, we isolated peripheral blood via submandibular vein puncture. Flow cytometric analysis showed that administration of DTx resulted in approximately 80% depletion of CD11b $^{+}$Ly6C^{+} cells (both Ly6C^{Lo} and Ly6C^{Hi} cells) for 24 to 36 hours following injection (►Fig. 2A, B). With time, the circulating Mo/MΦs returned. Peripheral blood neutrophil counts (CD11b^{+}Ly6G^{+}) and percentages were not affected by DTx injection in CD11b-DTR mice (►Fig. 2C, D). Importantly, DTx injection in CD11b-DTR mice did not have a significant effect on several measures of platelet function or the inflammatory phenotype (►Supplementary Figs. S1 and ►S2, available in the online version).

Reduction of CD11b^{+}Ly6C^{+} Mo/MΦs Does Not Significantly Affect Venous Thrombogenesis

We next determined how depletion of CD11b^{+}Ly6C^{+} Mo/MΦs impacted thrombogenesis. Mo/MΦs were depleted by DTx administration 24 hours prior to VT creation, and then IVC/thrombus was analyzed at 24 and 48 hours post-IVC ligation. We found no difference in thrombus size at 48 hours in DTx-treated mice, when compared with NaCl-treated controls in two models of VT (►Fig. 3A, 48-hour data shown). Similarly, there was no difference at 24 hours (thrombus weight to length 0.01797 ± 0.001209, $n = 7$ NaCl vs. 0.0181 ± 0.002248, $n = 7$, $p = 0.96$, stasis model, data not shown). In mice undergoing venous stasis, there was no significant difference in fibrin content detected by Picro-Mallory staining (►Fig. 3B, C) or by Western immunoblotting(►Fig. 3D). As Mo/MΦs may serve as a direct source of the plasminogen activator, urokinase-type plasminogen activator (uPA), or indirectly activate plasminogen via MMPs, we measured intrathrombus levels of plasminogen (►Fig. 3E) and found no difference between the two groups. To evaluate neutrophil recruitment and/or neutrophil extracellular traps (NETs) release, we measured cit-H_3 by Western immunoblotting (►Fig. 3F) and identified Ly6G+ intrathrombus PMNs by immunohistochemistry and found no difference between the two groups (►Fig. 3G-I). While we cannot draw the conclusion that Mo/MΦs do not contribute to venous thrombogenesis, these data suggest that significant reduction of circulating Mo/MΦs does not greatly alter qualitative thrombus formation.

DTx-Mediated Mo/MΦ Depletion Results in Impaired Venous Thrombosis Resolution by Selective Reduction of CD11b^{+}Ly6C^{Lo} Mo/MΦs

We next evaluated whether depleting circulating CD11b^{+} Mo/MΦs following stasis VT would affect thrombus resolution. Unlike thrombogenesis, which is thought to be largely mediated by platelets, cellular adhesion molecules, PMNs, and erythrocytes in a cooperative fashion, the main cellular component in the resolving thrombus is the Mo/MΦ.[16,37,38] To allow for normal circulating cellular milieu during thrombogenesis, CD11b^{+} Mo/MΦ depletion was initiated by intraperitoneal injection of DTx (or NaCl) after formation of

maximal thrombus size at 48 hours following IVC ligation and mice were reinjected every 48 hours thereafter until harvest. To confirm adequate depletion of $CD11b^+$ Mo/MΦs in thrombus and make comparisons with previously established proportions of $CD11b^+Ly6C^{Hi}$ and $CD11b^+Ly6C^{Lo}$ Mo/MΦs in WT mice, IVC/thrombi were harvested at day 8 for flow cytometry and cell quantification. A significant decrease in IVC/thrombus $CD11b^+Ly6C^{Lo}$ Mo/MΦ counts was observed (►Fig. 4A), with no change in $CD11b^+Ly6C^{Hi}$ Mo/MΦ counts (►Fig. 4B). Simultaneously, the relative percentages of $CD11b^+Ly6G^+$ neutrophils at day 8 were not different in the IVC/thrombus (►Fig. 4C). A reduction of proreparative Mo/MΦs was confirmed with immunohistochemical staining of Arg1 (antigen marker of $CD11b^+Ly6C^{Lo}$ Mo/MΦs) demonstrated a paucity of positively staining cells in the DTx-treated mice (►Fig. 4D).

Thrombus resolution in mice with selective depletion of $CD11b^+Ly6C^{Lo}$ Mo/MΦs was grossly impaired (►Fig. 4E). DTx alone did not influence thrombus resolution in WT mice treated in an identical fashion compared with treatment with NaCl (C57Bl/6 mice with NaCl treatment 0.017 g/cm ± 0.002 vs. with DTx treatment 0.015 ± 0.002, $n = 6–8$, $p = 0.37$). As a confirmatory experiment, a second technique of Mo/MΦ depletion using clodronate micelle injection confirmed these findings in C57BL/6J mice. $CD11b^+Ly6C^+$ Mo/MΦs were depleted by approximately 30% in the treated mice compared with controls (liposomal micelle injections alone 42% ± 4 vs. clodronate lysosomes 30% ± 3, $p = 0.06$). A similar phenotype was observed with significantly impaired thrombus resolution at day 8 (►Supplementary Fig. S3, available in the online version).

To explore the Mo/MΦ function altered by loss of $CD11b^+Ly6C^{Lo}$ subset, we evaluated intrathrombus fibrinolysis, neovascularization, and clearance of necrotic cells. Monocytes/macrophages can serve as a direct source of the plasminogen activator uPA and can indirectly serve to activate plasminogen; thus, we measured intrathrombus plasminogen and found it to be decreased by approximately 50% in the mice with fewer $CD11b^+Ly6C^{Lo}$ Mo/MΦs (►Fig. 4F). Correspondingly, serum plasminogen was reduced by 40%, (NaCl 8.66 ± 1.90 ng/mL, DTx 5.19 ± 2.09 ng/mL, $n = 5–7$/group, $p = 0.25$). These findings correlated with a nonsignificant 40% decrease in fibrin deposition (►Fig. 4G). TAT levels did not differ between the two groups (NaCl 44.3 ± 12.4 vs. DTx 32.3 ± 4.7 ratio to β-actin, $n = 6–7$, $p = 0.40$). Assessment of the thrombosed vein for gene and protein expression of certain factors associated with thrombus resolution showed several trends in proinflammatory factor reduction with DTx-treated CD-11b-DTR mice, and significantly decreased IFN-γ protein levels (►Supplementary Figs. S4 and S5, available in the online version). Thrombus recanalization, as measured by vWF positively stained channels, was not affected by Mo/MΦ depletion (►Fig. 4H). Necrotic cells, as measured by TUNEL staining, did not differ between the two groups (21.8 ± 11.3 vs. 18.9 ± 7.0 pixels/hpf, $n = 5–7$, $p = 0.46$) suggesting no impairment in cellular debris clearance in the treated mice.

Adoptive Transfer of $CD11b^+Ly6C^{Lo}$ Mo/MΦs Reverses Impaired VT Resolution in Mo/MΦ Depleted Mice

To determine the direct effects of repopulating intrathrombus $CD11b^+Ly6C^{Lo}$ Mo/MΦs, we subjected the CD11b-DTR mice to the same DTx dosing protocol as above with Mo/MΦ

depletion beginning at 48 hours after thrombus creation. We then performed adoptive transfer via tail vein injection of FACS sorted $CD11b^{+}Ly6C^{Lo}$ Mo/MΦs (1×10^{6} cells) or RPMI vehicle control at 72 hours postthrombosis (24 hours post-DTx injection), with specimen harvest at day 8 (►Fig. 5A). To confirm the presence of the adoptively transferred cells in the IVC/thrombus of our experimental mice, we used $tdTomato^{+}$ red $ROSA^{mT/mG}$ donor cells and processed IVC/thrombus for flow cytometric analysis (►Fig. 5B). The relative percentages of $CD11b^{+}Ly6C^{Lo}$ cells did not differ between NaCl:RPMI treated controls and DTx:$Ly6C^{Lo}$ injected adoptive transfer mice (►Fig. 5C). Adoptive transfer of these $CD11b^{+}LyC6^{Lo}$ Mo/MΦs improved VT resolution in DTx-treated mice, with a significant reduction in thrombus size, as compared with RPMI vehicle-injected DTx-treated mice (►Fig. 5D).

Discussion

In this report, we show that a reduction of circulating $CD11b^{+}Ly6C^{+}$ monocytes does not appear to greatly impact qualitative venous thrombogenesis in two separate murine models. A reduction of the end effector Mo/MΦ ($CD11b^{+}Ly6C^{Lo}$ Mo/MΦ) does, however, significantly affect normal VT resolution. Moreover, $CD11b^{+}Ly6C^{Lo}$ Mo/MΦs are seemingly critical for this process, with adoptive transfer of these cells reversing the impaired resolution phenotype.

Multiple contributing factors to experimental venous thrombogenesis have been identified including chemokines, vWF, NETs, platelets, high mobility group box protein 1, and mast cell degranulation, among others.[5,7,8,17,18,39-41] Early cellular involvement of myeloid cells in either prothrombotic or antithrombotic roles is likely model dependent.[37,42] While others have shown Mo/MΦs may participate invenous thrombogenesis,[37] the $CD11b^{+}Ly6C^{+}$ monocyte cell lineage has not been thoroughly investigated directly in this model to date. We used the two most common models of VT, the IVC stasis and stenosis techniques, and found that > 80% $CD11b^{+}Ly6C^{+}$ depletion did not alter experimental thrombus formation as measured by VT size, fibrin, $Ly6G^{+}$ cells, and NETs markers. Consistent with the lack of effect on thrombogenesis was no effect of DTx-mediated depletion on circulating platelets, and several measures of platelet function.

Our data are also consistent with prior work in $CCR2^{-/-}$ mice, with no effect on VT size at day 2, suggesting a limited role for infiltrating Mo/MΦs in thrombogenesis.[11] Granted, even with this strongly suggestive data, it is not possible to completely exclude a role of Mo/MΦs in thrombogenesis as we did not completely ablate $CD11b^{+}Ly6C^{+}$ cells with approximately 20% remaining as determined by flow cytometry. Interestingly, these findings are in contrast to other myeloid-lineage cells such as neutrophils which have been shown to contribute to pathologic VT via nuclear decondensation and NET formation,[40] and mast cells which have been shown to induce thrombosis via Weibel–Palade body secretion following histamine degranulation in the vein wall.[41]

This data supports the paradigm that VT resolution is similar to wound healing with infiltrating blood monocyte-derived macrophages characterized by an early preponderance of $CD11b^{+}Ly6C^{Hi}$ inflammatory Mo/MΦs followed by a staged predominance of

proreparative CD11b^{+}Ly6C^{Lo} Mo/MΦs.[24,25,43] It is likely, as has been previously shown,[25,43] that the CD11b^{+}Ly6C^{Hi} Mo/MΦs convert to CD11b^{+}Ly6C^{Lo} Mo/MΦs in the resolving thrombus. The DTx method of depletion was associated with greater depletion of proreparative CD11b^{+}Ly6C^{Lo} Mo/MΦs by DTx administration, as has been demonstrated in other models.[44] The underlying reason for the phenomenon is unclear. It may be that the conversion of LyC6^{Hi} to LyC6^{Lo} is impaired or delayed in the setting of DTx-mediated depletion.[45,46] Alternatively, although intrathrombus LyC6^{hi} were not significantly fewer at 8 days, we speculate they may have been reduced at earlier time points, as the LyC6^{Hi} are the first to be released from both the bone marrow and extramedullary sources.

As increased proportions of CD11b^{+}Ly6C^{Hi} Mo/MΦs have been associated with augmented inflammation and impaired wound healing in diabetes models,[25] it may be expected that increased proportion of CD11b^{+}Ly6C^{Hi} Mo/MΦs to the decreased CD11b^{+}Ly6C^{Lo} Mo/MΦs resulted in delayed VT resolution. These data and others suggest a prolonged proinflammatory state is maladaptive, and results in impaired VT resolution. We have hypothesized that this may be driven by the local cytokine milieu generated by these cells.[25,43] We found IFN-γ was reduced in the thrombosed vein tissue in DTx-depleted mice, suggesting this is downstream from the Mo/MΦ-mediated activities. Prior work from our laboratory suggested IFN- γ was important in modulating MMP activity and early VT resolution.[11] Our findings here are corroborated by supplement prior work by Schönfelder et al, who demonstrated through a similar model that a reduction of IVC/thrombus neutrophils and a shift to CD11b^{+}Gr-1^{-} (CD11b^{+}Ly6C^{Lo}) Mo/MΦs resulted in accelerated VT resolution.[35]

We explored several myeloid cell-mediated mechanisms of VT resolution in experimental models of stasis VT.[5,6] We found the primary difference was significantly reduced plasminogen levels in CD11b^{+}Ly6C^{Lo} Mo/MΦ-depleted mice compared with controls. This is supported by Singh et al, whereby uPA$^{-/-}$ mice had significantly larger VT, and they reversed the impaired VT resolution using a bone marrow chimera strategy, correlating with increased thrombus Mo/MΦs.[20] Others have shown that CCR2^{+} cells (CD11b^{+}Ly6C^{Hi}) mediate fibrin clearance in a plasminogen-dependent manner—consistent with our data showing significantly larger thrombi and decreased plasminogen.[47]

We were surprised to find no difference in VT neovascularization and apoptosis, given that CCR2$^{-/-}$ mice[15] demonstrated larger thrombi with decreased vWF + channels.[11] This phenomenon may be due to mouse genotype, differing myeloid cell influx based on chemotactic factors, or that a more dramatic depletion of myeloid cells is necessary to see the effect. Alternatively, since a significant portion of CD11b^{+}Ly6C^{Hi} cells remained in the thrombus in our model, these cells may direct neovascularization as well as other mechanisms of sterile inflammation.[14] These conclusions are supported by data from Nosaka et al, who demonstrated that IVC/thrombus Mo/MΦs are responsible for the secretion of MMP9 and vascular endothelial growth factor-α which contribute to VT resolution and neovascularization and this is highly dependent on the IFN-γ pathway.[48] More investigation into the subtle functional differences in Mo/MΦ subsets is required to determine their discrete roles in VT resolution and neovascularization.

Important unanswered questions remain; first, does the Mo/MΦ influx direct the vein wall fibrosis that is inherent in VT resolution and is it the driver of postthrombotic syndrome? Preliminary data at a 14-day time point in the stasis model suggests reduced fibrosis following $CD11b^{+}Ly6C^{Lo}$ Mo/MΦ depletion, as determined by trichrome histologic measures (unpublished data). Consistent with this observation, $CCR2^{-/-}$ mice demonstrate reduced vein wall injury at day 21.[30] Second, does the mechanism of thrombogenesis determine Mo/MΦ phenotype? From prior work in an electrolytic induction model (EIM),[16] IVC thrombus Mo/MΦs seem to take on a more proinflammatory phenotype in a stasis model when compared with a flow model (IVC stenosis/EIM). Lastly, the translation of these data suggests that promoting a transition from $CD11b^{+}Ly6C^{Hi}$ to $CD11b^{+}Ly6C^{Lo}$ Mo/MΦs in resolving thrombus could improve VT resolution; either by blocking $CD11b^{+}Ly6C^{Hi}$ Mo/MΦ influx, transforming $CD11b^{+}Ly6C^{Hi}$ cells to $CD11b^{+}Ly6C^{Lo}$ cells, or by blocking $CD11b^{+}Ly6C^{Lo}$ Mo/MΦ efflux.

In summary, $CD11b^{+}Ly6C^{+}$ monocytes do not overtly impact venous thrombogenesis but their terminal effector cell $CD11b^{+}Ly6C^{Lo}$ Mo/MΦs are essential for normal VT resolution, perhaps mediated via IFN-γ-directed proteolytic activity. Future investigations in this line of research may unveil novel targets for new, nonanticoagulant, immunotherapies for DVT/PE.

Supplementary Material

Refer to Web version on PubMed Central for supplementary material.

Acknowledgments

Funding

This work was supported by the NIH: R01HL132988–03; T32HL076123–14 and Jobst Foundation grant from the American Venous Forum.

Conflict of Interest

P.H. reports grants from NIH, T32HL076123–14, grants from NIH, R01HL132988–03, during the conduct of the study. A.S.K. reports grants from NIH, T32HL076123–14, grants from Jobst Foundation, American Venous Forum, during the conduct of the study.

References

1. Anderson FA Jr, Wheeler HB, Goldberg RJ, et al. A population-based perspective of the hospital incidence and case-fatality rates of deep vein thrombosis and pulmonary embolism. The Worcester DVT Study. Arch Intern Med 1991;151(05):933–938 [PubMed: 2025141]
2. Kearon C, Akl EA, Ornelas J, et al. Antithrombotic therapy for VTE disease: CHEST guideline and expert panel report. Chest 2016;149(02):315–352 [PubMed: 26867832]
3. Weitz JI, Bates SM. New anticoagulants. J Thromb Haemost 2005;3(08):1843–1853 [PubMed: 16102051]
4. Di Nisio M, van Es N, Büller HR. Deep vein thrombosis and pulmonary embolism. Lancet 2016;388(10063):3060–3073 [PubMed: 27375038]
5. Wakefield TW, Myers DD, Henke PK. Mechanisms of venous thrombosis and resolution. Arterioscler Thromb Vasc Biol 2008;28(03):387–391 [PubMed: 18296594]
6. Swystun LL, Liaw PC. The role of leukocytes in thrombosis. Blood 2016;128(06):753–762 [PubMed: 27354721]

7. Saha P, Humphries J, Modarai B, et al. Leukocytes and the natural history of deep vein thrombosis: current concepts and future directions. Arterioscler Thromb Vasc Biol 2011;31(03):506–512 [PubMed: 21325673]
8. Budnik I, Brill A. Immune factors in deep vein thrombosis initiation. Trends Immunol 2018;39(08):610–623 [PubMed: 29776849]
9. Henke PK, Varga A, De S, et al. Deep vein thrombosis resolution is modulated by monocyte CXCR2-mediated activity in a mouse model. Arterioscler Thromb Vasc Biol 2004;24(06):1130–1137 [PubMed: 15105284]
10. Laser A, Elfline M, Luke C, et al. Deletion of cysteine-cysteine receptor 7 promotes fibrotic injury in experimental post-thrombotic vein wall remodeling. Arterioscler Thromb Vasc Biol 2014;34(02):377–385 [PubMed: 24311382]
11. Henke PK, Pearce CG, Moaveni DM, et al. Targeted deletion of CCR2 impairs deep vein thrombosis resolution in a mouse model. J Immunol 2006;177(05):3388–3397 [PubMed: 16920980]
12. Henke PK, Mitsuya M, Luke CE, et al. Toll-like receptor 9 signaling is critical for early experimental deep vein thrombosis resolution. Arterioscler Thromb Vasc Biol 2011;31(01):43–49 [PubMed: 20966396]
13. Kessinger CW, Kim JW, Henke PK, et al. Statins improve the resolution of established murine venous thrombosis: reductions in thrombus burden and vein wall scarring. PLoS One 2015;10(02):e0116621 [PubMed: 25680183]
14. Nathan C, Ding A. Nonresolving inflammation. Cell 2010;140(06):871–882 [PubMed: 20303877]
15. Ali T, Humphries J, Burnand K, et al. Monocyte recruitment in venous thrombus resolution. J Vasc Surg 2006;43(03):601–608 [PubMed: 16520180]
16. Gallagher KA, Obi AT, Elfline MA, et al. Alterations in macrophage phenotypes in experimental venous thrombosis. J Vasc Surg Venous Lymphat Disord 2016;4(04):463–471 [PubMed: 27639001]
17. Fuchs TA, Brill A, Duerschmied D, et al. Extracellular DNA traps promote thrombosis. Proc Natl Acad Sci U S A 2010;107(36):15880–15885 [PubMed: 20798043]
18. Stark K, Philippi V, Stockhausen S, et al. Disulfide HMGB1 derived from platelets coordinates venous thrombosis in mice. Blood 2016;128(20):2435–2449 [PubMed: 27574188]
19. Chang CF, Goods BA, Askenase MH, et al. Erythrocyte efferocytosis modulates macrophages towards recovery after intracerebral hemorrhage. J Clin Invest 2017
20. Singh I, Burnand KG, Collins M, et al. Failure of thrombus to resolve in urokinase-type plasminogen activator gene-knockout mice: rescue by normal bone marrow-derived cells. Circulation 2003;107(06):869–875 [PubMed: 12591758]
21. Henke PK, Varma MR, Moaveni DK, et al. Fibrotic injury after experimental deep vein thrombosis is determined by the mechanism of thrombogenesis.Thromb Haemost 2007;98(05):1045–1055 [PubMed: 18000610]
22. Murray PJ, Allen JE, Biswas SK, et al. Macrophage activation and polarization: nomenclature and experimental guidelines. Immunity 2014;41(01):14–20 [PubMed: 25035950]
23. Jablonski KA, Amici SA, Webb LM, et al. Novel markers to delineate murine M1 and M2 macrophages. PLoS One 2015;10(12):e0145342 [PubMed: 26699615]
24. Arnold L, Henry A, Poron F, et al. Inflammatory monocytes recruited after skeletal muscle injury switch into antiinflammatory macrophages to support myogenesis. J Exp Med 2007;204(05):1057–1069 [PubMed: 17485518]
25. Kimball A, Schaller M, Joshi A, et al. Ly6C^{Hi} blood monocyte/macrophage drive chronic inflammation and impair wound healing in diabetes mellitus. Arterioscler Thromb Vasc Biol 2018;38(05):1102–1114 [PubMed: 29496661]
26. Diaz JA, Obi AT, Myers DD Jr, et al. Critical review of mouse models of venous thrombosis. Arterioscler Thromb Vasc Biol 2012;32(03):556–562 [PubMed: 22345593]
27. Stoneman V, Braganza D, Figg N, et al. Monocyte/macrophage suppression in CD11b diphtheria toxin receptor transgenic mice differentially affects atherogenesis and established plaques. Circ Res 2007;100(06):884–893 [PubMed: 17322176]

28. Diaz JA, Wrobleski SK, Alvarado CM, et al. P-selectin inhibition therapeutically promotes thrombus resolution and prevents vein wall fibrosis better than enoxaparin and an inhibitor to von Willebrand factor. Arterioscler Thromb Vasc Biol 2015;35(04):829–837 [PubMed: 25657307]
29. Culmer DL, Dunbar ML, Hawley AE, et al. E-selectin inhibition with GMI-1271 decreases venous thrombosis without profoundly affecting tail vein bleeding in a mouse model. Thromb Haemost 2017;117(06):1171–1181 [PubMed: 28300869]
30. Dewyer NA, El-Sayed OM, Luke CE, et al. Divergent effects of Tlr9 deletion in experimental late venous thrombosis resolution and vein wall injury. Thromb Haemost 2015;114(05):1028–1037 [PubMed: 26179893]
31. Gallagher KA, Joshi A, Carson WF, et al. Epigenetic changes in bone marrow progenitor cells influence the inflammatory phenotype and alter wound healing in type 2 diabetes. Diabetes 2015;64(04):1420–1430 [PubMed: 25368099]
32. Auffray C, Sieweke MH, Geissmann F. Blood monocytes: development, heterogeneity, and relationship with dendritic cells. Annu Rev Immunol 2009;27:669–692 [PubMed: 19132917]
33. Nahrendorf M, Swirski FK, Aikawa E, et al. The healing myocardium sequentially mobilizes two monocyte subsets with divergent and complementary functions. J Exp Med 2007;204(12):3037–3047 [PubMed: 18025128]
34. Zigmond E, Varol C, Farache J, et al. Ly6C hi monocytes in the inflamed colon give rise to proinflammatory effector cells and migratory antigen-presenting cells. Immunity 2012;37(06):1076–1090 [PubMed: 23219392]
35. Schönfelder T, Brandt M, Kossmann S, et al. Lack of T-bet reduces monocytic interleukin-12 formation and accelerates thrombus resolution in deep vein thrombosis. Sci Rep 2018;8(01):3013 [PubMed: 29445199]
36. Cailhier JF, Partolina M, Vuthoori S, et al. Conditional macrophage ablation demonstrates that resident macrophages initiate acute peritoneal inflammation. J Immunol 2005;174(04):2336–2342 [PubMed: 15699170]
37. von Brühl ML, Stark K, Steinhart A, et al. Monocytes, neutrophils, and platelets cooperate to initiate and propagate venous thrombosis in mice in vivo.J Exp Med 2012;209(04):819–835 [PubMed: 22451716]
38. Deroo S, Deatrick KB, Henke PK. The vessel wall: a forgotten player in post thrombotic syndrome. Thromb Haemost 2010;104(04):681–692 [PubMed: 20694280]
39. Kimball AS, Obi AT, Diaz JA, Henke PK. The emerging role of NETs in venous thrombosis and immunothrombosis. Front Immunol 2016;7:236 [PubMed: 27446071]
40. Martinod K, Demers M, Fuchs TA, et al. Neutrophil histone modification by peptidylarginine deiminase 4 is critical for deep vein thrombosis in mice. Proc Natl Acad Sci U S A 2013;110(21):8674–8679 [PubMed: 23650392]
41. Ponomaryov T, Payne H, Fabritz L, Wagner DD, Brill A. Mast cells granular contents are crucial for deep vein thrombosis in mice. Circ Res 2017;121(08):941–950 [PubMed: 28739590]
42. Henke PK, Varma MR, Deatrick KB, et al. Neutrophils modulate post-thrombotic vein wall remodeling but not thrombus neovascularization. Thromb Haemost 2006;95(02):272–281 [PubMed: 16493489]
43. Dal-Secco D,Wang J, Zeng Z, et al. A dynamic spectrum of monocytes arising from the in situ reprogramming of CCR2+ monocytes at a site of sterile injury. J Exp Med 2015;212(04):447–456 [PubMed: 25800956]
44. Perego C, Fumagalli S, Zanier ER, et al. Macrophages are essential for maintaining a M2 protective response early after ischemic brain injury. Neurobiol Dis 2016;96:284–293 [PubMed: 27697537]
45. Rahman K, Vengrenyuk Y, Ramsey SA, et al. Inflammatory Ly6Chi monocytes and their conversion to M2 macrophages drive atherosclerosis regression. J Clin Invest 2017;127(08):2904–2915 [PubMed: 28650342]
46. Crane MJ, Daley JM, van Houtte O, Brancato SK, Henry WL Jr, Albina JE. The monocyte to macrophage transition in the murine sterile wound. PLoS One 2014;9(01):e86660 [PubMed: 24466192]

47. Motley MP, Madsen DH, Jürgensen HJ, et al. A CCR2 macrophage endocytic pathway mediates extravascular fibrin clearance in vivo. Blood 2016;127(09):1085–1096 [PubMed: 26647393]

48. Nosaka M, Ishida Y, Kimura A, et al. Absence of IFN-γ accelerates thrombus resolution through enhanced MMP-9 and VEGF expression in mice. J Clin Invest 2011;121(07):2911–2920 [PubMed: 21646723]

What is known about this topic?

- Ly6C+ peripheral blood monocytes differentiate into $Ly6C^{Hi}$ (proinflammatory) $Ly6C^{Lo}$ (prohealing) during wound healing and inflammatory states.
- Monocytes/macrophages are the primary leukocyte involved in the process of VT resolution, but role of distinct subtypes is unknown.

What does this paper add?

- Monocyte/macrophage depletion does not affect normal thrombogenesis, but does result in impaired thrombus resolution.
- In “take away and give back” experiments, $Ly6C^{Lo}$ monocyte/macrophage subtype is found to be essential to venous thrombus resolution.

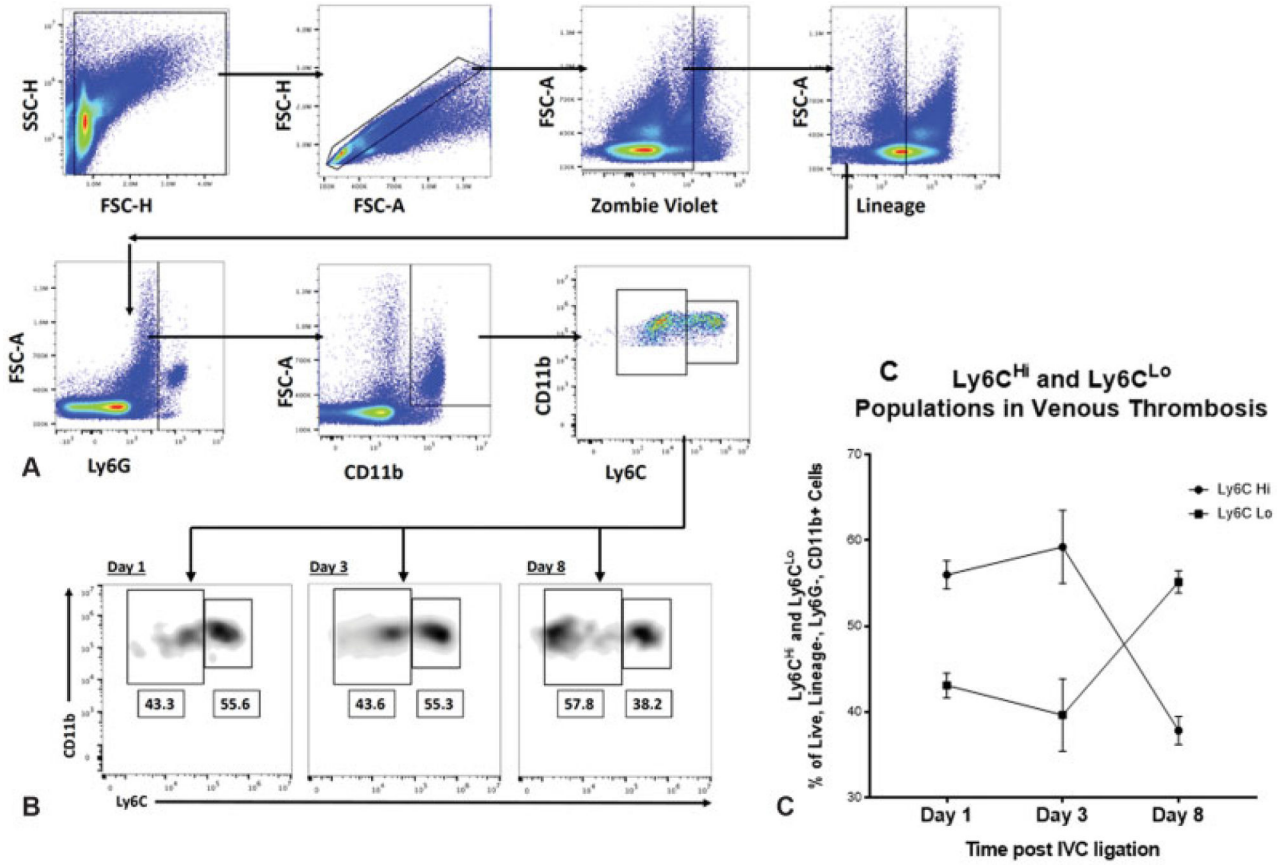

Fig. 1.

Quantitative flow cytometry methodology to determine proportions and counts of CD11b $^{+}$Ly6C^{Hi} and CD11b^{+}Ly6C^{Lo} monocyte/macrophages (Mo/MΦs) in inferior vena cava (IVC)/thrombus following formation of venous thrombosis. (**A**) Gating strategy to isolate CD11b^{+}Ly6C^{Hi} and CD11b^{+}Ly6C^{Lo} Mo/MΦs for quantification. (**B**) Density plots and (**C**) line graph of proportions of CD11b^{+}Ly6C^{Hi} and CD11b^{+}Ly6C^{Lo} Mo/MΦs in C57BL/6 mice at days 1, 3, and 8 following the stasis model of venous thrombosis (n = 5 per group, repeated once).

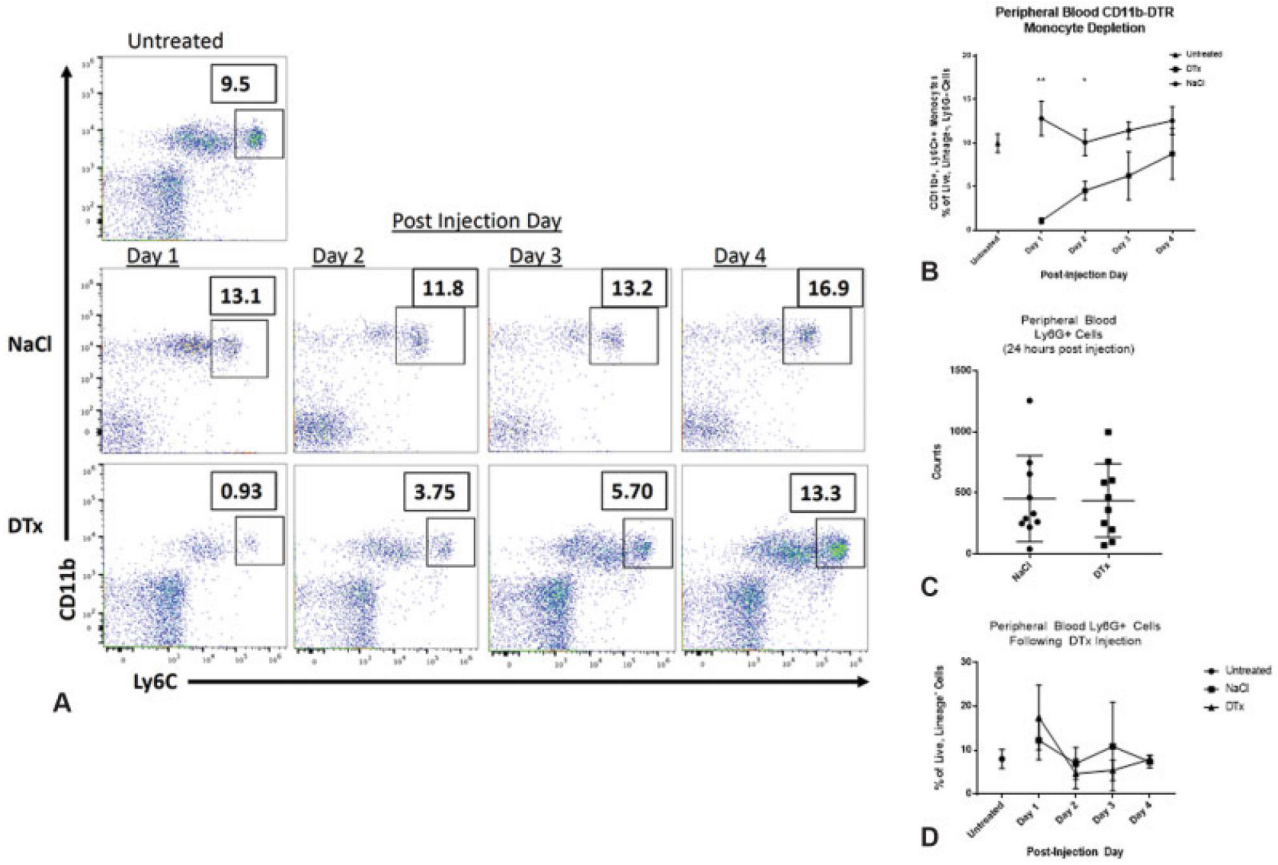

Fig. 2.

CD11b-diphtheria toxin receptor (DTR)/diphtheria toxoid (DTx) depletion timeline in peripheral blood $CD11b^{+}Ly6C^{2+}$ monocytes. (**A**) Pseudo-color plots of $CD11b^{+}Ly6C^{+}$ peripheral blood monocytes untreated, treated with NaCl, or treated with DTx (10 ng/g) at days 1–4 post-DTx injection. (**B**) Monocyte depletion timeline following treatment with DTx ($n = 6$ per group, repeated twice, $*p < 0.05$, $**p < 0.01$). (**C**) Circulating peripheral blood $CD11b^{+}Ly6G^{+}$ neutrophil counts by flow cytometry 24 hours post-DTx injection ($n =$ 10 per group, repeated once, NS). (**D**) Circulating peripheral blood $CD11b^{+}Ly6G^{+}$ neutrophil timeline following DTx injection ($n = 6$ per group, repeated once, all time points NS).

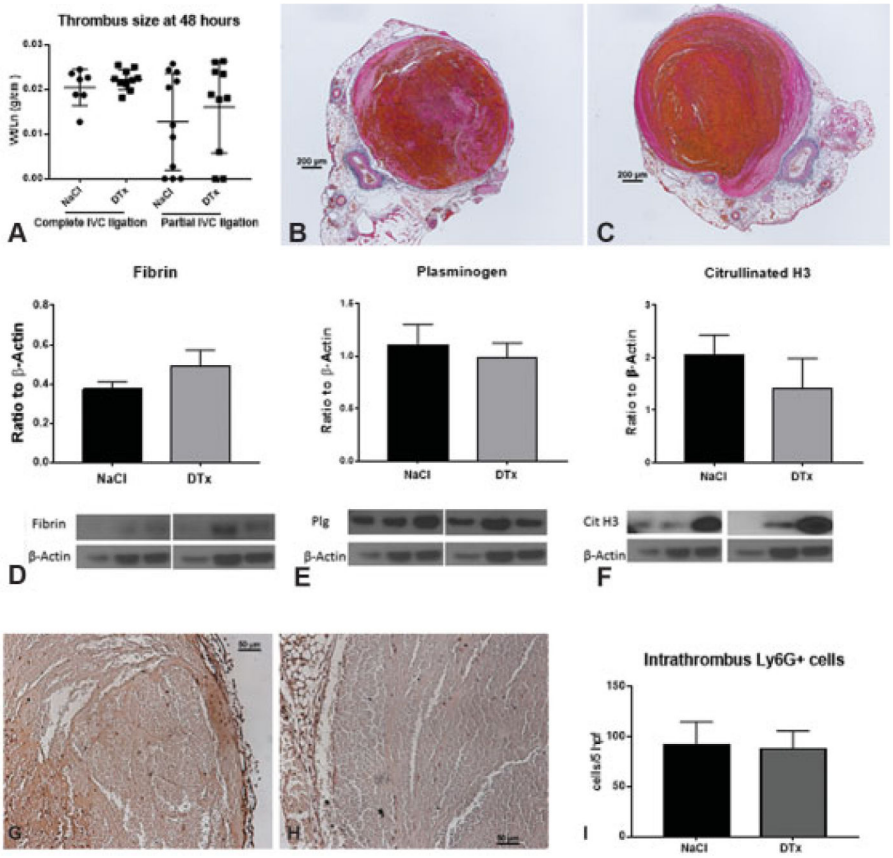

Fig. 3.

Predepletion of circulating $CD11b^{+}Ly6C^{+}$ monocyte/macrophages does not affect qualitative or quantitative thrombus formation by the stasis model of venous thrombosis (VT). Inferior vena cava (IVC) thrombus size (weight-to-length ratio [g/cm]) at (**A**) 48 hours following stasis (complete IVC ligation) and stenosis (partial IVC ligation) induced thrombosis (n = 7–10 per group, repeated once, all p-values = NS). Representative photo of thrombus in (**B**) NaCl and (**C**) diphtheria toxoid (DTx)-treated CD11b-diphtheria toxin receptor (DTR) mice at 4× with Picro-Mallory stain (fibrin stains red; red blood cells [RBCs] stain yellow; connective tissue stains blue, both photos of thrombus formed under completed IVC ligation). Levels of IVC thrombus (**D**) fibrin, (**E**) plasminogen, and (**F**) citrullinated H3 by Western immunoblotting at 48 hours normalized by ratio to β-actin with representative blots (n = 7–10 per group, repeated once, all p-values = NS). Representative immunohistochemical staining pictures of Ly6G+ neutrophils in (**G**) NaCl and (**H**) DTx-treated mice at 2 days post-thrombosis (complete IVC ligation model). (**I**) Intrathrombus Ly6G cell counts at 2 days post-thrombosis (n = 6–7 per group, NS).

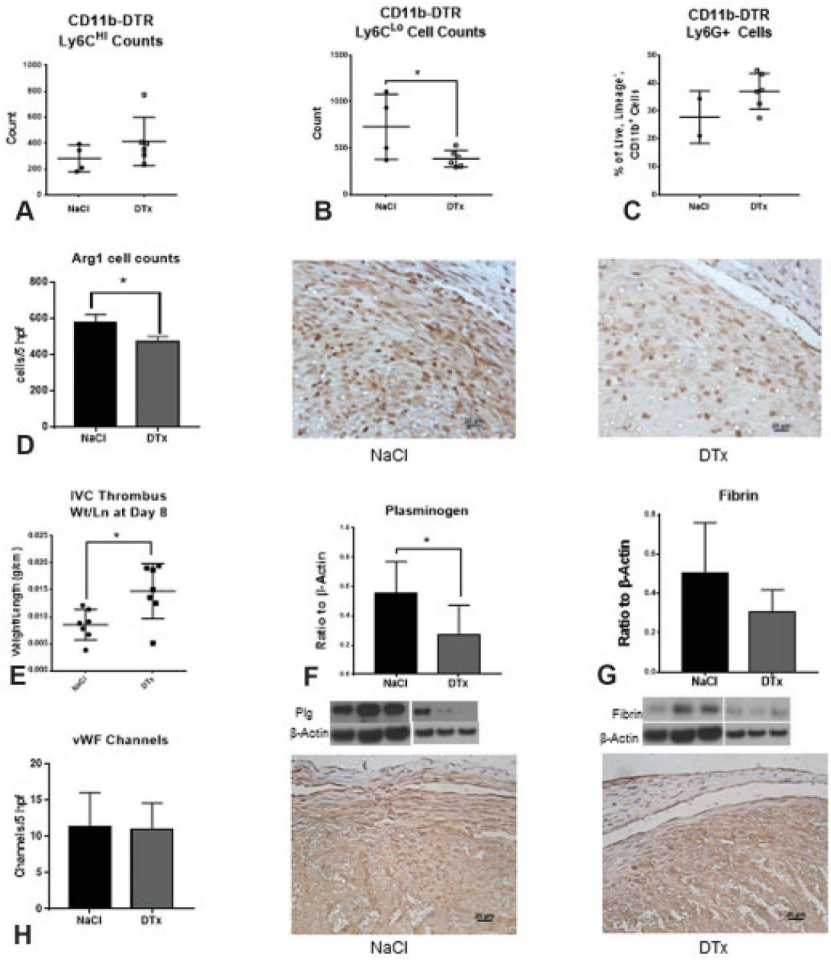

Fig. 4.

Depletion of inferior vena cava (IVC)/thrombus Mo/MΦs following stasis venous thrombosis depletes $CD11b^{+}Ly6C^{Lo}$ Mo/MΦs and impairs venous thrombus resolution. (**A**) $CD11b^{+}Ly6C^{Hi}$ and (**B**) $CD11b^{+}Ly6C^{Lo}$ Mo/MΦ counts by flow cytometry in IVC/thrombus in NaCl and diphtheria toxoid (DTx)-treated CD11b-diphtheria toxin receptor (DTR) mice at day 8 poststasis thrombosis ($n = 4$–6 per group, repeated once, $*p < 0.05$). (**C**) $CD11b^{+}Ly6G^{+}$ neutrophils expressed as a percentage of $CD11b^{+}$ cells in IVC/thrombus in NaCl and DTx-treated CD11b-DTR mice at day 8 poststasis thrombosis ($n = 2$–6 per group [2 controls expired], NS). (**D**) Histogram of Arg1 positively staining cells in the IVC/thrombus with representative immunohistochemical staining at 20× of Arg1 + cells ($n = 3$–4 per group, repeated once, $*p < 0.05$). (**E**) IVC/thrombus weight-to-length ratio (g/cm) at day 8 in CD11b-DTR mice treated with NaCl or DTx ($n = 7$ per group, repeated once, $*p < 0.05$). (**F**) Levels of IVC thrombus plasminogen and (**G**) fibrin by Western immunoblotting with representative blots ($n = 6$ per group, repeated once, $*p < 0.05$). (**H**) Cell counts of von Willebrand factor (vWF) positively staining cells ($n = 4$, p = ns) and representative photomicrographs at 40× ($n = 4$ per group, NS).

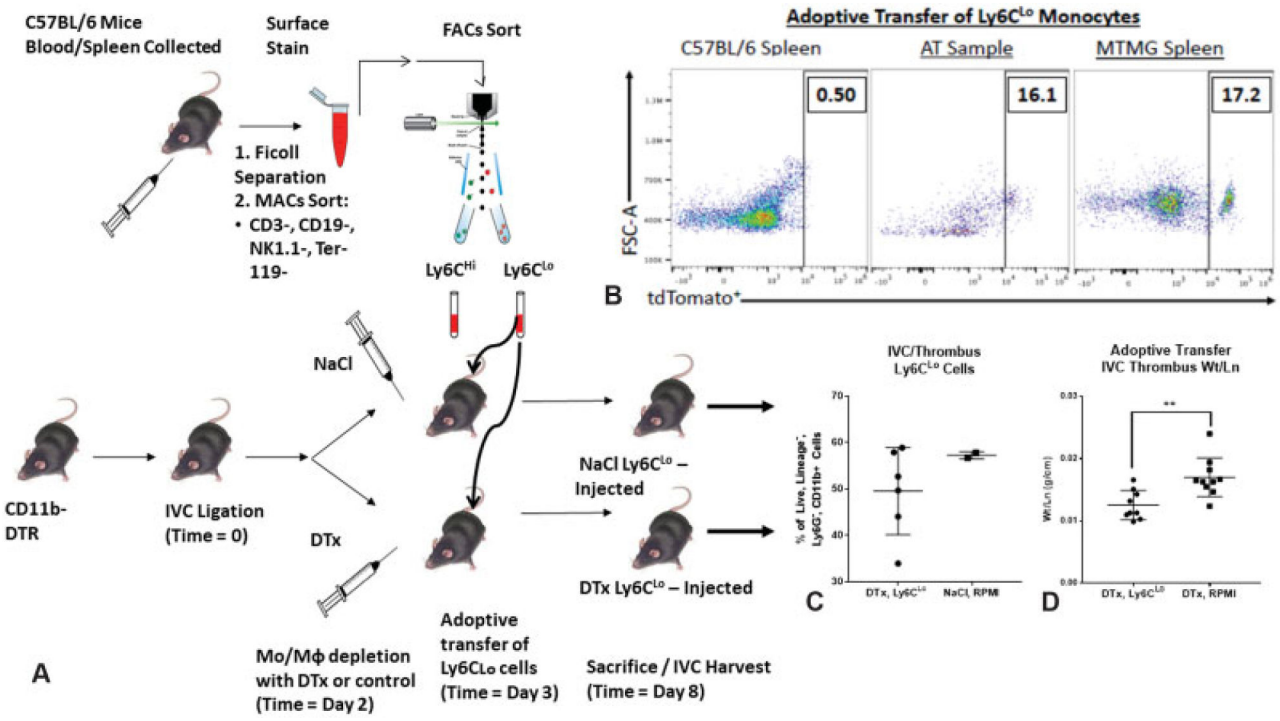

Fig. 5.

Impaired venous thrombosis (VT) resolution is reversible with adoptive transfer of $CD11b^{+}$ $Ly6C^{Lo}$ monocytes. (**A**) Schematic of experimental protocol with inferior vena cava (IVC) ligation at time 0, monocyte/macrophage depletion at day 2, harvest of $CD11b^{+}Ly6C^{Lo}$ cells ($n = 30$), and adoptive transfer on day 3, with harvest of thrombus and vein wall on day 8. (**B**) Pseudo-color plots of adoptively transferred $tdtomato^{+}CD11b^{+}Ly6C^{Lo}$ monocyte/macrophages in recipient CD11b-diphtheria toxin receptor (DTR) mice with positive and negative controls (AT, adoptive transfer). (**C**) IVC/thrombus $CD11b^{+}Ly6C^{Lo}$ cells expressed as a percentage of live, $lineage^{-}$, $Ly6G^{-}$, $CD11b^{+}$ cells in NaCl + RPMI injected and diphtheria toxoid (DTx) + 1×10^{6} $CD11b^{+}Ly6C^{Lo}$ cell injected mice at day 8 post-VT ($n =$ 2–6 per group [2 controls expired], NS). (**D**) IVC/thrombus weight-to-length ratio at day 8 in CD11b-DTR mice treated with DTx followed by adoptive transfer of 1×10^{6} $CD11b^{+}Ly6C^{Lo}$ cells or RPMI Vehicle 24 hours following initial DTx injection ($n = 10$ per group; representative of two independent experiments; $^{**}p < 0.01$).